SPANDIDOS PUBLICATIONS

ONCOLOGY LETTERS 28: 296, 2024

Targeting CCR3 with antagonist SB 328437 sensitizes 5-fluorouracil-resistant gastric cancer cells: Experimental evidence and computational insights

ÁLVARO GUTIÉRREZ[1,2], MARÍA ELENA REYES[3], CAROLINA LARRONDE[3], PRISCILLA BREBI[1,2,4] and BÁRBARA MORA-LAGOS[3]

[1]Laboratory of Integrative Biology, Centro de Excelencia en Medicina Traslacional, Scientific and Technological Bioresource Nucleus, Universidad de La Frontera, 4810296 Temuco, Chile; [2]Millennium Institute on Immunology and Immunotherapy, Scientific and Technological Bioresource Nucleus, Universidad de La Frontera, 4810296 Temuco, Chile; [3]Instituto de Ciencias Biomédicas, Facultad de Ciencias de la Salud, Universidad Autónoma de Chile, 4810101 Temuco, Chile; [4]Biomedical Research Consortium - Chile, Scientific and Technological Bioresource Nucleus, Universidad de La Frontera, 4810296 Temuco, Chile

Received November 29, 2023; Accepted April 10, 2024

DOI: 10.3892/ol.2024.14429

Abstract. Gastric cancer (GC) ranks fifth globally in cancer diagnoses and third for cancer-related deaths. Chemotherapy with 5-fluorouracil (5-FU), a primary treatment, faces challenges due to the development of chemoresistance. Tumor microenvironment factors, including C-C motif chemokine receptor 3 (CCR3), can contribute to chemoresistance. The present study evaluated the effect of CCR3 receptor inhibition using the antagonist SB 328437 and the molecular dynamics of this interaction on resistance to 5-FU in gastric cancer cells. The 5-FU-resistant AGS cell line (AGS R-5FU) demonstrated notable tolerance to higher concentrations of 5-FU, with a 2.6-fold increase compared with the parental AGS cell line. Furthermore, the mRNA expression levels of thymidylate synthase (TS), a molecular marker for 5-FU resistance, were significantly elevated in AGS R-5FU cells. CCR3 was shown to be expressed at significantly higher levels in these resistant cells. Combining SB 328437 with 5-FU resulted in a significant decrease in cell viability, particularly at higher concentrations of 5-FU. Furthermore, when SB 328437 was combined with 5-FU at a high concentration, the relative mRNA expression levels of CCR3 and TS decreased significantly. Computational analysis of CCR3 demonstrated dynamic conformational changes, especially in extracellular loop 2 region, which indicated potential alterations in ligand recognition. Docking simulations demonstrated that SB 328437 bound to the allosteric site of CCR3, inducing a conformational change in ECL2 and hindering ligand recognition. The present study provides comprehensive information on the molecular and structural aspects of 5-FU resistance and CCR3 modulation, highlighting the potential for therapeutic application of SB 328437 in GC treatment.

Correspondence to: Dr Bárbara Mora-Lagos, Instituto de Ciencias Biomédicas, Facultad de Ciencias de la Salud, Universidad Autónoma de Chile, 01690 Avenida Alemania, 4810101 Temuco, Chile
E-mail: barbara.mora@uautonoma.cl

Key words: CC chemokine receptor-3, chemoresistance, 5-fluorouracil, computational biology, molecular dynamics, allosteric binding, antagonist

Introduction

Gastric cancer (GC) is the fifth most frequently diagnosed cancer and the third highest cause of cancer-related deaths around the world (1). Diagnosis often occurs in advanced or metastatic stages, and the primary treatment strategy is chemotherapy based on the combination of platinum drugs and 5-fluorouracil (5-FU) (2). Acting as a pyrimidine antagonist, 5-FU inhibits DNA replication by competing with uracil for binding to thymidylate synthase (TS) (3). The clinical application of 5-FU is limited by the development of chemoresistance after chemotherapy (4,5). Molecular mechanisms involved in chemoresistance to 5-FU include increased DNA damage repair, regulation of membrane drug transporters, dysregulation of transcription factors (e.g., overexpression of EIF5A2, FOXM1 and GPC4, or downregulation of RanBPM and TFAP2C) and tumor microenvironment (TME) factors such as cancer-associated fibroblast (CAFs), endothelial-1 and aquaporin 1 (5). The TME comprises CAFs, mesenchymal cells and immune components, such as tumor-associated macrophages (TAM), which secrete cytokines and chemokines that contribute to chemoresistance (6). In this context, chemokine receptors, such as C-C motif chemokine receptor 3 (CCR3), are possible therapeutic targets. CCR3 has G protein associated transmembrane regions and is mainly expressed by eosinophils and other immune cells (7). CCR3 can bind numerous ligands with activator functions [chemokine (C-C motif) ligand (CCL) 3, 4, 5, 7, 13, 15, 23, 24, 26 and 28] and others as antagonists (CCL9, 10, 18), as well as CCL11 which has a dual function (7). Several of these ligands have been reported to be associated with chemoresistance in cancer,

including CCL5, CCL11 and CCL15 (6), and our previous study reported overexpression of CCL5 in cisplatin-resistant gastric cancer cells (8). Furthermore, CCR3 expression has been reported in certain cancers such as renal (9), colon (10) and, head and neck (11). In patients with GC, CCR3 expression has been previously reported in peripheral blood CD4+ lymphocytes (12). There are several CCR3 antagonists/inhibitors, including SB 297006 and SB 328437. SB 328437 is a potent and highly selective inhibitor of CCR3 and has been reported to have attenuated spontaneous chronic colitis in mice, reducing the number of eosinophils and regulatory molecules in the colon (13). Furthermore, SB 328437 has been reported to have reversed resistance to pazopanib and inhibited lung metastasis in a renal clear cell carcinoma model (14). Computational biology has contributed to the development of understanding of the interaction between chemokines and their ligands. X-ray crystallography techniques have revealed the three-dimensional configurations of several chemokines, including CCR5, CCR2 and CCR3 (15). Although variations in the quaternary structure have been observed, the monomeric unit, probably the key functional form of CCR2 and CCR3 (15), remains conserved. Although the effect of SB 328437 has been reported at the cellular level (16), the specific interaction of SB 328437 with CCR3 and its associated with resistance to 5-FU in GC has not been elucidated. The present study evaluated the effect of CCR3 receptor inhibition using the antagonist SB 328437 and assessed the molecular dynamics of this interaction on resistance to 5-FU in GC cells. In this study, a novel 5-FU-resistant gastric cancer cell line was established and validated through viability assays and TS gene-targeted RT-qPCR. The impact of CCR3 receptor inhibition by SB 328437 and its molecular dynamism on 5-FU resistance were investigated. Bioinformatics analysis utilized a closely related CCR5 structure to predict CCR3 binding site, refined within a stable membrane environment, and assessed ligand binding stability and receptor conformational changes.

Materials and methods

Chemicals. The chemotherapeutic agent, 5-FU was purchased from Selleck Chemicals and reconstituted at a concentration of 3.3 mM in DMSO. The CCR3 antagonist, SB 328437, was purchased from MedChemExpress and reconstituted at a concentration of 10 mM in DMSO.

Cells and culture. The gastric adenocarcinoma AGS cell line was purchased from the European Collection of Authenticated Cell Cultures. The mycoplasma-free status of the parental cell line was confirmed using the LookOut Mycoplasma PCR Detection Kit (Sigma-Aldrich; Merck KGaA). Cells were grown in RPMI-1640 medium supplemented with 10% (v/v) fetal bovine serum (Thermo Fisher Scientific, Inc.) and 1% (v/v) penicillin and streptomycin (Thermo Fisher Scientific, Inc.) and maintained at 37˚C in a 95% humidified atmosphere and 5% CO_2 conditions. Cells were subcultured at 70-80% confluence and harvested after treatment with 0.25% trypsin and 0.02% EDTA (Corning, Inc.).

Development of 5-FU resistant AGS cells. AGS parental cells were used to establish 5-FU-resistant AGS cells (AGS R-5FU) by stepwise increases in 5-FU drug doses according to the method previously reported by Coley (17). Briefly, the starting treatment dose was set at 20% of the half maximal effective concentration (EC_{50}) of the parental cells (17). Drug doses were gradually increased until an arbitrarily defined resistance index (RI) ≥2 was reached. RI values were calculated by dividing the EC_{50} values of resistant cells by the EC_{50} values of parental cells. Once the cells acquired 5-FU resistance, they were grown in a drug-free medium for two weeks, frozen in liquid nitrogen and then awakened in a medium containing 5-FU to confirm the level of chemoresistance.

RNA extraction and quantitative analysis. The mRNA expression levels of TS, a molecular marker involved in 5-FU resistance (4) and CCR3, were quantified using reverse transcription-quantitative (RT-q) PCR. Total RNA was extracted from ~2.0×10^6 cells using TRIzol (Thermo Fisher Scientific, Inc.) according to the manufacturer's instructions. RNA concentration was determined using the Infinite® NanoQuant spectrophotometer (Tecan Group, Ltd.), and integrity was evaluated by measuring RNA 260/280 absorbance ratio and gel electrophoresis. The RNA was then treated with DNase I (Promega Corporation) at 37˚C for 30 min and pre-incubated with 500 μg/ml random primers (Promega Corporation), followed by denaturation at 70˚C for 10 min. The first-strand complimentary cDNA was prepared from 1 μg of RNA in a total reaction volume of 20 μl using 25 mM dNTPs (Promega Corporation), RNasin ribonuclease inhibitor (Promega Corporation), 200 U/μl M-MLV reverse transcriptase (Promega Corporation) and M-MLV reverse transcriptase 5X buffer (Promega Corporation) at 37˚C for 45 min. Subsequently, cDNA was amplified by qPCR using Brilliant II Ultra-Fast SYBR® Green qPCR Master Mix according to the manufacturer's protocol, using the Stratagene Mx-3000p real-time PCR system (Agilent Technologies, Inc.). The RT-qPCR included an initial denaturation step at 95˚C for 10 min to ensure DNA denaturation. Amplification comprised 40 cycles, consisting of denaturation at 95˚C for 15 sec, annealing at 60˚C for 30 sec and extension at 72˚C for 30 sec. Subsequently, a melting curve was performed to assess amplification specificity. The initial temperature was 95˚C for 15 sec, followed by a stage at 55˚C for 1 min, with a gradual temperature increase of 0.15˚C per sec until 95˚C was reached. Relative mRNA expression levels were determined using the $2^{-\Delta\Delta Cq}$ method (18), using ACTB as the reference gene. Primer sequences used in the present study are presented in Table SI.

Cell viability assays. The viability of cells treated with 5-FU and/or SB 328437 was performed using a standard viability assay (MTT-formazan assay). Briefly, 4×10^3 cells were seeded in 96-well plates in 100 μl of culture medium and incubated at 37˚C for 24 h to allow cell attachment. Cells were exposed to the treatment agents for 72 h at different pharmacological concentrations: firstly, 0.01 to 1,000 μM 5-FU was used for the determination of EC_{50} values and then, these values were used alone or in combination with 50 μM SB 328437 to evaluate the effects of SB 328437 on resistance to 5-FU. Cells treated with DMSO (vehicle) were used as controls. After 72 h of incubation, the culture medium was removed and the cells were washed with 100 μl Dulbecco's PBS/Modified (Thermo Fisher

Scientific, Inc.) and were subsequently treated with MTT at 0.5 mg/ml, followed incubation at 37˚C for 2 h. Absorbance was measured at 570 nm wavelength using an Infinite NanoQuant spectrophotometer (Tecan Group, Inc.).

Protein preparation. The CCR3 crystal structure contains seven transmembrane α-helices and an eighth α-helix in the intracellular domain. The initial structure of CCR3 was obtained from the Protein Data Bank (PDB) (19) database (PDB ID, 7X9Y). The membrane environment, composed of 1-palmitoyl-2-oleoyl-sn-glycero-3-phosphocholine, was generated using the CHARMM-GUI server v3.8 (2-4). The CHARMM force field parameters for SB328437 were acquired from the 'Ligand Reader and Model' tool on the CHARMM-GUI web server (20-22). The system underwent restraint in the xyz plane with a harmonic potential gradient, starting from 4,000 kJ/mol/nm^2 in the initial NVT equilibration step and reducing to 50 kJ/mol/nm^2 in the final NPT equilibration step. Subsequently, production runs were conducted without any restraint for a duration of 100 ns.

Docking methodology. Autodock 4.2 (23) was used to model docking *in silico*, employing the Lamarckian genetic algorithm. The docking site was chosen based on the relative position of well-studied CCR receptor structures, following the CCR5-Maraviroc crystallographic structure (PDB: 4MBS). This docking region, situated closer to the extracellular loops (ECL1, ECL2 and ECL3), was selected, as it has been reported that binding sites for other molecules are typically located in this region (24). The docking active site was treated as a rigid molecule, while ligands were considered flexible, with all non-ring torsions deemed active. Cluster analysis was conducted after the docking experiment to identify the global minimum conformation of SB 328437 in the potential CCR3 binding site. The ligand poses with all-atoms root mean square deviation <0.1 nm, were clustered, ranked by their lowest docking energy and the representative binding mode was selected. The 10 poses with lowest energy were chosen for further investigation.

Simulation parameters. Molecular dynamics (MD) simulations were executed using GROMACS software v.2019 (25) under periodic boundary conditions. The minimization step comprised 50,000 steps with an emtol of 100 kJ/mol/nm. Equilibration steps were divided into NVT and NPT equilibration, with temperature coupling to T=310 K using the Berendsen thermostat. Pressure coupling utilized the Berendsen barostat with a semi-isotropic coupling scheme. Non-bonded interactions were computed as Lennard-Jones potentials, and electrostatics were calculated as Coulomb interactions. For the production run, electrostatic and non-bonded interactions were computed using the equilibration method, but temperature and pressure coupling schemes were changed to Nose-Hoover and Parrinello-Rahman, respectively. LINCS constraints for H-bonds were applied at each step, and a time step of 2 fsec was used.

Principal component analysis (PCA) calculation. PCA was performed using GROMACS as previously described (26). Briefly, GROMACS utilities gmx_covar and gmx_anaeig were used for PCA of CCR3-Alone and CCR3-SB328437 complexes based on 100 ns MD simulations. The first two eigenvectors with the largest eigenvalues were used to create a 2D projection of independent trajectories to better understand the conformational behavior pattern.

Image rendering. The Visual Molecular Dynamics (VMD) software package (23) was used to extract and calculate the data used for image rendering and the Protein Imager webserver was used to render the data (27).

Statistical analysis. All experiments were performed in biological and technical triplicates for each condition. Data were analyzed using GraphPad Prism 10.0.3 (Dotmatics). EC_{50} values were calculated from dose-response curves using non-linear regression. RT-qPCR data were analyzed using the Mann-Whitney U test and the Kruskal-Wallis test with Dunn's post-hoc test. Cell viability assays were analyzed using the Kruskal-Wallis test with Dunn's post-hoc test. P<0.05 was considered to indicate a statistically significant difference. Mean values are presented with a 95% confidence interval.

Results

Establishment of 5-FU-resistant AGS cells. Dose-response curves of parental and chemo-resistant AGS cells are presented (Fig. 1A). The dose-response curves allowed EC_{50} values to be obtained for AGS WT and AGS R-5FU cell lines. The EC_{50} value for AGS R-5FU was 24.8 μM ±0.75, which represented a 2.6-fold resistance index (RI) compared with the AGS WT (EC_{50}=9.7 μM ±0.23). In addition, a significant increase in the relative expression of TS (P<0.05) was observed in AGS R-5FU cells compared with AGS WT (Fig. 1B).

CCR3 is overexpressed in 5-FU-resistant AGS cells. RT-qPCR was used to evaluate the transcriptional expression of *CCR3* in AGS R-5FU and AGS WT cells (Fig. 1C). This demonstrated that CCR3 mRNA expression levels were significantly higher in AGS R-5FU cells compared with AGS WT cells (P<0.05).

CCR3 antagonist in combination with 5-FU decreases cell viability and the relative expression of CCR3 and TS in 5-FU-resistant AGS cells. MTT assays were performed in AGS R-5FU cells treated with the CCR3 antagonist, SB 328437, and/or 5-FU to evaluate their effect on cell viability (Fig. 1D). No significant differences in cell viability were demonstrated between cells treated with SB 328437 and control cells. However, a substantial decrease in cell viability was observed when SB 328437 was combined with 5-FU; cells treated with SB 328437 combined with 9.7 μM 5-FU demonstrated a significant reduction in cell viability compared with control cells (P<0.0001) and cells treated with 9.7 μM of 5-FU only (P<0.01). Similarly, when SB 328437 was combined with 24.8 μM 5-FU, cell viability was significantly reduced when compared with control cells (P<0.0001), and cells treated with SB 328437 only (P<0.001).

The transcriptional expression of CCR3 and TS in AGS R-5FU cells treated for 72 h with SB 328437 and/or 5-FU. There were no significant differences in the relative expression

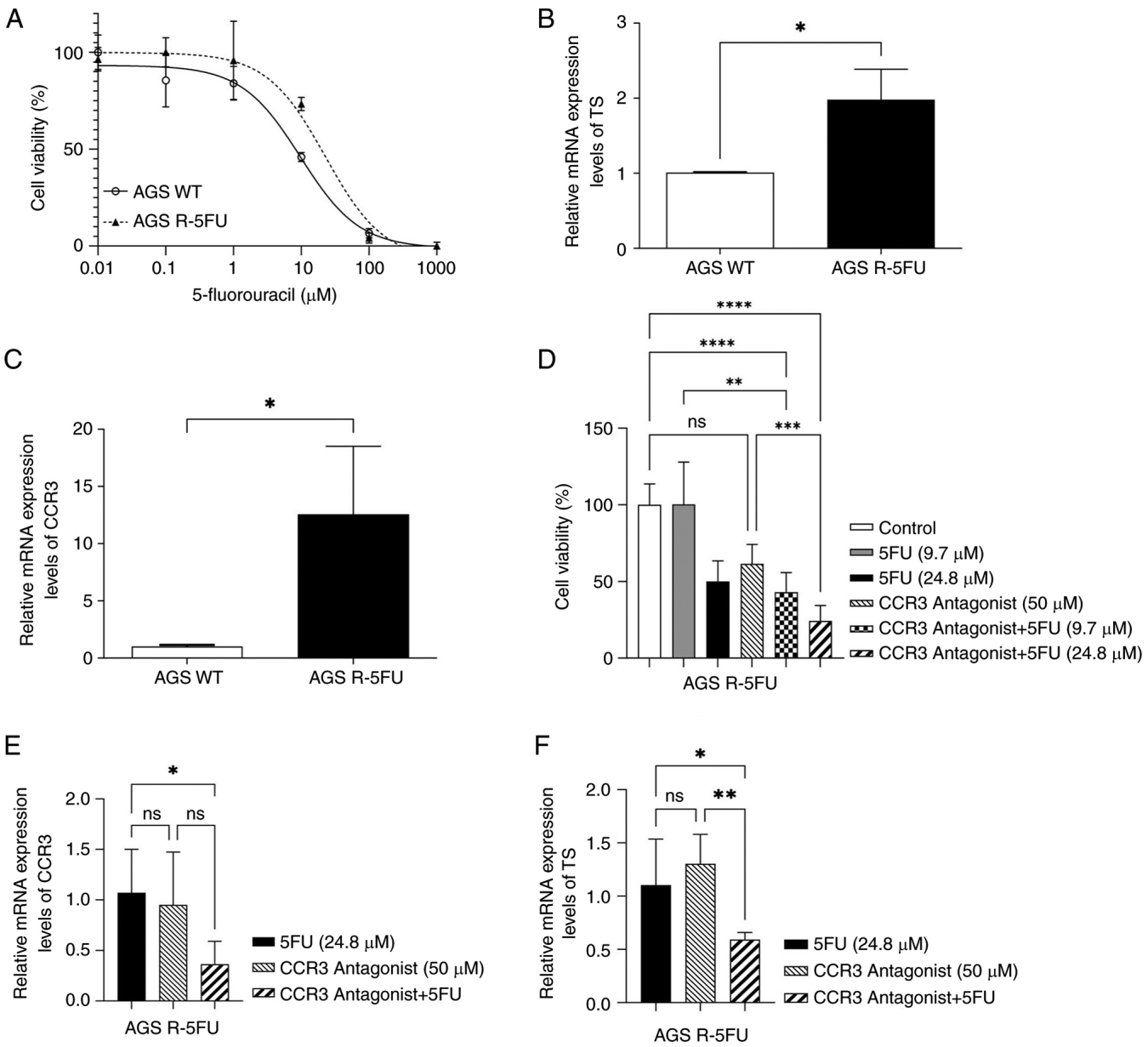

Figure 1. *In vitro* assays. (A) Dose-response curves for AGS R-5FU and AGS WT. mRNA expression levels of (B) TS and (C) CCR3 in AGS R-5FU and AGS WT. (D) Cell viability of AGS R-5FU cells treated with 5-FU and/or CCR3 antagonist, SB 328437, for 72 h. mRNA expression levels of (E) CCR3 and (F) TS after treatment with SB 328437 and/or 5-FU. Data were expressed as mean ± standard deviation of three biological replicates. *P<0.05, **P<0.01, ***P<0.001 and ****P<0.0001. AGS WT, wild type AGS cells; 5FU, 5-fluorouracil; AGS R-5FU, 5-FU resistant AGS cells; TS, thymidylate synthase; CCR3, C-C motif chemokine receptor 3; ns, not significant.

of CCR3 between cells treated with SB 328437 and those treated with 24.8 μM 5-FU. However, when SB 328437 was combined with 5-FU, a significant decrease in the mRNA expression level of CCR3 was demonstrated compared with the 5-FU group (P<0.05; Fig. 1E). Similarly, a significant reduction in the relative expression of TS was observed in cells treated with the SB 328437/5-FU combination compared to those exposed to 5-FU (P<0.05) or SB 328437 (P<0.01) alone (Fig. 1F).

Changes in the structure of wild-type CCR in the open/close states. To propose transition states, it is necessary to identify cyclical changes in the system. These opening and closing states can be observed as transitional microstates between the opening of the binding pocket and its closure. The conformational differences between the opening and closing of the binding pocket were presented (Fig. 2A).

The receptor transition cycle, between opening and closing, appears to be related to the proximity of the amino acids which belong to the N-terminal region to the ECL2 loop, with a role also indicated for ECL3 and TM5. For the structure of CCR3 to change to its completely closed state, amino acids N271 and Y193 must be oriented toward each other which results in their interaction; this interaction generates a displacement of the extracellular ECL3 region towards the binding pocket of CCR3 functioning as a gate, which closes the possibility of interaction with any ligand. However, for the 'closed' transition microstate to be maintained over time, the Y193-N271

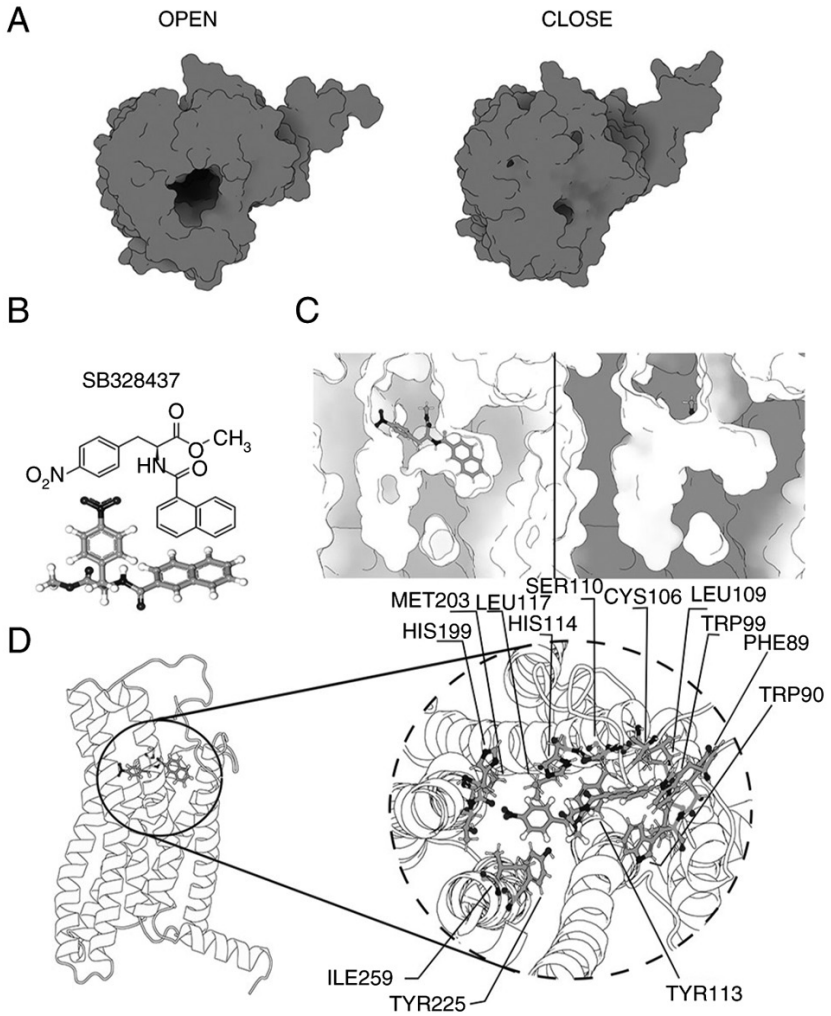

Figure 2. Structural model of CCR3. (A) Structures of CCR3 generated *in silico*, highlighting Open and Close state. Structures are represented as surfaces seen from above. (B) The structure of SB 328437. (C) Binding site of CCR3 with SB 328437 located. (D) Common residues involved in ligand binding, these correspond mainly to hydrophobic residues, with certain residues, such as cysteine 106 and 183, involved in ligand recognition.

interaction must be supported by another region of CCR3, the N-terminal region. For a 'closed' microstate to be fully achieved it is necessary for the N-terminal region of CCR3, characterized by its alanine residue, to be oriented toward the extracellular ECL2 loop. This orientation establishes an interaction between A31 and E181, blocking the capacity of the N-terminal region as 'ligand recognition', which is known to be the region responsible for the identification of possible ligands.

SB 328437 binds to the allosteric site of CCR3 and blocks the entrance of endogenous ligands. To understand the interaction between CCR3 and SB 328437, a docking, guided specifically for the allosteric region of CCR3, was performed to visualize a normal ligand relocation at the specific site (Fig. 2B). During each of the molecular dynamics performed the SB 328437 ligand was positioned within the allosteric site of CCR3. CCR3 could be characterized by 2 binding pockets, site A where the recognition site for CCL3 or any CCR3 ligand is located and site B (where SB 328437 is bound), which would correspond to the allosteric site (Fig. 2C). Given the conformational shift of ECL2 that follows its contact and anchoring to the CCR3 allosteric site-which is strikingly similar to the previously proposed change in the closed microstate-this binding has notable implications for the potential impact of SB 328437 on CCR3.

The major conformational change visualized in CCR3 following the binding of SB 328437 is found in the ECL2 region, which is repositioned, closing the passage to the N-terminal region and the binding pocket, blocking the recognition of any ligand. This conformational change occurs after ~50 nsec and is characterized by the interaction between the ligand and, the ECL2 and N-terminal regions. This interaction occurs through a punctual interaction of cysteine 183, which belongs to the ECL2 region, and leucine 32, which belongs to the N-terminal region. Both residues are oriented towards the ligand, initiating the conformational change, blocking ligand recognition, and closing the receptor opening.

SB 328437 possesses 2 aromatic rings and as such, it needs a highly hydrophobic binding site to interact with CCR3. This is demonstrated in the internal region of CCR3 which can be characterized by the hydrophobic residues A31, L32, L87, C106, L109, S110, C183, I259, S262 and S263, which can be

seen to be distributed around the binding site and so can be expected to support the interaction of the binding site with the ligand. Another feature of SB 328437 is the large number of atoms that can act as proton donors or acceptors, these attract residues such as T86, F89, W90, W99, Y113 and T200; interactions which hold the ligand in place and ultimately affect the structure of CCR3. The formation of an environment that makes possible the interaction, understood as recognition and stabilization of the ligand inside the binding pockets, is possible by the composition of highly hydrophobic residues that generate a favorable environment, supported lately by the interaction between the ligand and the charged residues. Even if these residues promote a favorable environment for ligand stabilization, specific residues generate strong interactions with the ligand and keep the structure stabilized, which can be seen in Fig. 2D.

Discussion

Although 5-FU is the chemotherapy treatment of first choice for advanced GC, its effectiveness is limited by chemoresistance (28). In the present study, a new 5-FU-resistant GC cell line (AGS R-5FU) was developed, the RI of which, as well as the overexpression of the TS gene, made it possible to confirm the acquisition of resistance. This study was initiated with two 5FU-resistant gastric cancer cell lines, AGS R-5FU and MKN-28 R-5FU. However, as it was not possible to confirm the overexpression of TS in MKN-28 R-5FU, its use was discontinued. Consequently, the utilization of only a single resistant cell line represents a limitation of the present study.

As 5-FU exerts its anticancer effects through the inhibition of TS and causing misincorporation of bases into DNA and RNA, overexpression of TS is considered the main molecular mechanism of resistance to 5-FU (4). CCR3, a chemokine receptor expressed by eosinophils and other immune cells, has been identified in peripheral blood $CD4^+$ lymphocytes of patients with GC. This clinical study reveals a positive regulatory relationship between the expression of CCR5 and CCR3, indicating a complex interaction between these molecules in the immune response linked to cancer progression (12). Furthermore, some of the ligands of CCR3, such as CCL5, have been reported to be associated with chemoresistance (6,8). However, the inhibition of CCR3 by the antagonist SB 328437 has been reported to reverse resistance to pazopanib (14). The inhibition of CCR3 in 5-FU-resistant GC has not been previously assessed. Chemokines are membrane proteins expressed in low quantities and as such, their detection by techniques such as western blotting is limited. Therefore, the present study focused on the transcriptional expression of CCR3. CCR3 was overexpressed in AGS R-5FU, and its inhibition using CCR3 antagonist, SB 328437, combined with 5-FU, triggered sensitization to 5-FU, decreasing cell viability. Jöhrer *et al* (9) proposed that CCR3 expression might facilitate proliferative responses of tumor cells and ligands of CCR3 in renal cell carcinoma. As CCR3 actives signaling pathways, such as MAPK and JAK/STAT, and affects migration, cell growth/differentiation and apoptosis (29), the inhibition of CCR3 could explain the decrease in cell viability. It was also observed that SB 328437 alone did not significantly decrease the transcriptional expression of CCR3 or the cell viability of AGS R-5FU cells. However, when SB 328437 was combined with 5-FU, the mRNA expression levels of CCR3 and cell viability both significantly decreased.

To the best of our knowledge, no previous studies have assessed the association of the combination of SB 328437 and 5-FU in drug chemoresistance. The present study evaluated whether this combination also influenced the transcriptional expression of TS. The results indicated that SB 328437 combined with 5-FU significantly decreased the expression of TS. As TS overexpression is a hallmark of chemoresistance to 5-FU, its inhibition served to confirm the reduction in levels of chemoresistance. The potential importance of these sensitization results necessitated the description of the mechanism of interaction between SB 328437 and CCR3, and so a computational biology analysis was performed. Computational biology techniques support the prediction and proposal of mechanisms of action for structures that have not yet been resolved, such as the interactions of chemokines with different ligands, as is the case of CCR3. Similar studies have been previously reported for CCR5, one of the most studied chemokines, which regulates the trafficking and functions of immune cells (30). *In-silico* analysis has shown that the upstream region of CCR5 and the extracellular loop ECL2 were identified as critical in the interaction of Maraviroc with relevant chemokine ligands (31). In the present study, a structural analysis was performed of the behavior of CCR3 with SB 328437, a ligand already known to be a selective receptor antagonist, but which lacked a description of its mechanism of interaction. The behavior of the CCR3-SB 328437 complex indicated a clear tendency toward conformational change that caused receptor blockade and promoted the displacement of the N-terminal region, relevant for ligand recognition, disabling the ligand recognition function of CCR3. In research related to CCRs, the functioning of CCR3 receptors has been described following the classical behavior of 2-site models. These refer to the relationship between an allosteric site and an orthosteric site in the recognition and modulation of conformational changes for the activation or inhibition of a structure (15). CCR3 is not exempt from this mechanism; based on the *in-silico* modelling of the interaction of CCR3 with SB 328437, the receptor changed conformation between open and closed, rendering the N-terminal region unable to exert its ligand recognition effect. The relevance of the N-terminal region has been described for most CCRs, identifying it as one of the most relevant and functionally conserved regions for this type of receptor (32). In addition to the relevance of the N-terminal region, similar results have been reported in relation to the relevance of ECL2 and ECL3 in ligand recognition by CCR3 (33). Both regions were modified by the effect of SB 328437 in the present study. Given the ability of CCR3 to be modulated through different recognition sites, the demonstrated of an allosteric activation is to be expected. Such allosteric modulation has been described by other researchers, who propose that in addition to allosteric modulation at the binding site, cholesterol has the effect of being an affinity modulator to different ligands (34,35). Thus, describing the possible allosteric binding site of SB 328437 allows us to progressively approach a comprehensive understanding of the mechanism of CCR3 activation. The results of the *in-silico* modeling interaction of CCR3 and SB 328437 support those of another investigation of CCR3 antagonists at the allosteric site (36), highlighting hydrophobic residues, which provide the correct environment for SB 328437 to interact with CCR3 and remain stable.

The present study demonstrated the impact of CCR3 on chemoresistance to 5-FU in GC, emphasizing the potential therapeutic effect of SB 328437. The structural changes observed suggest a novel approach to sensitizing cancer cells by targeting CCR3, presenting opportunities for further exploration in cancer therapy. Future studies to clarify the synergistic interaction between SB 328437 and 5-FU should be conducted using both *in vitro* and *in vivo* assays. This interaction should also be confirmed with the use of other CCR3 inhibitors, which would provide a more comprehensive perspective on the role of this possible therapeutic alternative in reducing drug resistance in GC.

Acknowledgements

The authors would like to thank Mr. Javier Retamal (Laboratory of Integrative Biology,Universidad de La Frontera) for their advice on the experimental design..

Funding

This work was supported by the National Research and Development Agency through the National Doctoral Scholarship (grant no. 21222011), FONDECYT Postdoctorado (grant no. 3210629), FONDECYT Regular (grant no. 1210440) and FONDEF Idea (grant no. ID21I10027) grants. This work was also supported by the Millennium Institute on Immunology and Immunotherapy IMII (grant nos. ICN09_016/ICN 2021_045; former P09/016-F) and CORFO BMRC, Biomedical research consortium-Chile.

Availability of data and materials

The data generated in the present study may be requested from the corresponding author.

Authors' contributions

AG and BML confirm the authenticity of all the raw data. AG, MER, CR, PB and BML designed the study. AG and BM-L conducted experiments. AG, MER, CR, PB and BML analyzed the data, designed the figures and wrote the manuscript. All authors read and approved the final manuscript.

Ethics approval and consent to participate

Not applicable.

Patient consent for publication

Not applicable.

Competing interests

The authors declare that they have no competing interests.

References

1. Sung H, Ferlay J, Siegel RL, Laversanne M, Soerjomataram I, Jemal A and Bray F: Global cancer statistics 2020: GLOBOCAN estimates of incidence and mortality worldwide for 36 cancers in 185 countries. CA Cancer J Clin 71: 209-249, 2021.
2. Ychou M, Boige V, Pignon JP, Conroy T, Bouché O, Lebreton G, Ducourtieux M, Bedenne L, Fabre JM, Saint-Aubert B, *et al*: Perioperative chemotherapy compared with surgery alone for resectable gastroesophageal adenocarcinoma: An FNCLCC and FFCD multicenter phase III trial. J Clin Oncol 29: 1715-1721, 2011.
3. Longley DB, Harkin DP and Johnston PG: 5-Fluorouracil: Mechanisms of action and clinical strategies. Nat Rev Cancer 3: 330-338, 2003.
4. Zhang N, Yin Y, Xu SJ and Chen WS: 5-Fluorouracil: Mechanisms of resistance and reversal strategies. Molecules 13: 1551-1569, 2008.
5. Sethy C and Kundu CN: 5-Fluorouracil (5-FU) resistance and the new strategy to enhance the sensitivity against cancer: Implication of DNA repair inhibition. Biomed Pharmacother 137: 111285, 2021.
6. Reyes ME, de La Fuente M, Hermoso M, Ili CG and Brebi P: Role of CC chemokines subfamily in the platinum drugs resistance promotion in cancer. Front Immunol 11: 901, 2020.
7. Zajkowska M and Mroczko B: Eotaxins and their receptor in colorectal cancer-a literature review. Cancers (Basel) 12: 1383, 2020.
8. Mora-Lagos B, Cartas-Espinel I, Riquelme I, Parker AC, Piccolo SR, Viscarra T, Reyes ME, Zanella L, Buchegger K, Ili C and Brebi P: Functional and transcriptomic characterization of cisplatin-resistant AGS and MKN-28 gastric cancer cell lines. PLoS One 15: e0228331, 2020.
9. Jöhrer K, Zelle-Rieser C, Perathoner A, Moser P, Hager M, Ramoner R, Gander H, Höltl L, Bartsch G, Greil R and Thurnher M: Up-regulation of functional chemokine receptor CCR3 in human renal cell carcinoma. Clin Cancer Res 11: 2459-2465, 2005.
10. Lee YS, Kim SY, Song SJ, Hong HK, Lee Y, Oh BY, Lee WY and Cho YB: Crosstalk between CCL7 and CCR3 promotes metastasis of colon cancer cells via ERK-JNK signaling pathways. Oncotarget 7: 36842-36853, 2016.
11. Huang WY, Lin YS, Lin YC, Nieh S, Chang YM, Lee TY, Chen SF and Yang KD: Cancer-associated fibroblasts promote tumor aggressiveness in head and neck cancer through chemokine ligand 11 and C-C motif chemokine receptor 3 signaling circuit. Cancers (Basel) 14: 3141, 2022.
12. Andalib A, Doulabi H, Hasheminia S, Maracy M and Rezaei A: CCR3, CCR4, CCR5, and CXCR3 expression in peripheral blood CD4+ lymphocytes in gastric cancer patients. Adv Biomed Res 2: 31, 2013.
13. Filippone RT, Dargahi N, Eri R, Uranga JA, Bornstein JC, Apostolopoulos V and Nurgali K: Potent CCR3 receptor antagonist, SB328437, suppresses colonic eosinophil chemotaxis and inflammation in the winnie murine model of spontaneous chronic colitis. Int J Mol Sci 23: 7780, 2022.
14. Wang C, Wang Y, Hong T, Cheng B, Gan S, Chen L, Zhang J, Zuo L, Li J and Cui X: Blocking the autocrine regulatory loop of Gankyrin/STAT3/CCL24/CCR3 impairs the progression and pazopanib resistance of clear cell renal cell carcinoma. Cell Death Dis 11: 117, 2020.
15. Shao Z, Tan Y, Shen Q, Hou L, Yao B, Qin J, Xu P, Mao C, Chen LN, Zhang H, *et al*: Molecular insights into ligand recognition and activation of chemokine receptors CCR2 and CCR3. Cell Discov 8: 44, 2022.
16. White JR, Lee JM, Dede K, Imburgia CS, Jurewicz AJ, Chan G, Fornwald JA, Dhanak D, Christmann LT, Darcy MG, *et al*: Identification of potent, selective non-peptide CC chemokine receptor-3 antagonist that inhibits eotaxin-, eotaxin-2-, and monocyte chemotactic protein-4-induced eosinophil migration. J Biol Chem 275: 36626-36631, 2000.
17. Coley HM: Development of drug-resistant models. Methods Mol Med 88: 267-274, 2004.
18. Livak KJ and Schmittgen TD: Analysis of relative gene expression data using real-time quantitative PCR and the 2(-Delta Delta C(T)) method. Methods 25: 402-408, 2001.
19. Berman HM, Westbrook J, Feng Z, Gilliland G, Bhat TN, Weissig H, Shindyalov IN and Bourne PE: The protein data bank. Nucleic Acids Res 28: 235-242, 2000.
20. Jo S, Kim T, Iyer VG and Im W: CHARMM-GUI: A web-based graphical user interface for CHARMM. J Comput Chem 29: 1859-1865, 2008.
21. Brooks BR, Brooks CL III, Mackerell AD Jr, Nilsson L, Petrella RJ, Roux B, Won Y, Archontis G, Bartels C, Boresch S, *et al*: CHARMM: The biomolecular simulation program. J Comput Chem 30: 1545-1614, 2009.

22. Wu EL, Cheng X, Jo S, Rui H, Song KC, Dávila-Contreras EM, Qi Y, Lee J, Monje-Galvan V, Venable RM, *et al*: CHARMM-GUI membrane builder toward realistic biological membrane simulations. J Comput Chem 35: 1997-2004, 2014.
23. Morris GM, Huey R, Lindstrom W, Sanner MF, Belew RK, Goodsell DS and Olson AJ: AutoDock4 and AutoDockTools4: Automated docking with selective receptor flexibility. J Comput Chem 30: 2785-2791, 2009.
24. Tan Q, Zhu Y, Li J, Chen Z, Han GW, Kufareva I, Li T, Ma L, Fenalti G, Li J, *et al*: Structure of the CCR5 chemokine receptor-HIV entry inhibitor maraviroc complex. Science 341: 1387-1390, 2013.
25. Berendsen HJC, van der Spoel D and van Drunen R: GROMACS: A message-passing parallel molecular dynamics implementation. Comput Phys Commun 91: 43-56, 1995.
26. Amadei A, Linssen AB and Berendsen HJ: Essential dynamics of proteins. Proteins 17: 412-425, 1993.
27. Tomasello G, Armenia I and Molla G: The protein imager: A full-featured online molecular viewer interface with server-side HQ-rendering capabilities. Bioinformatics 36: 2909-2911, 2020.
28. Xu ZY, Tang JN, Xie HX, Du YA, Huang L, Yu PF and Cheng XD: 5-Fluorouracil chemotherapy of gastric cancer generates residual cells with properties of cancer stem cells. Int J Biol Sci 11: 284-294, 2015.
29. Hembruff SL and Cheng N: Chemokine signaling in cancer: Implications on the tumor microenvironment and therapeutic targeting. Cancer Ther 7: 254-267, 2009.
30. Oppermann M: Chemokine receptor CCR5: Insights into structure, function, and regulation. Cell Signal 16: 1201-1210, 2004.
31. Salmas RE, Yurtsever M and Durdagi S: Investigation of inhibition mechanism of chemokine receptor CCR5 by micro-second molecular dynamics simulations. Sci Rep 5: 13180, 2015.
32. Wasilko DJ, Johnson ZL, Ammirati M, Che Y, Griffor MC, Han S and Wu H: Structural basis for chemokine receptor CCR6 activation by the endogenous protein ligand CCL20. Nat Commun 11: 3031, 2020.
33. Duchesnes CE, Murphy PM, Williams TJ and Pease JE: Alanine scanning mutagenesis of the chemokine receptor CCR3 reveals distinct extracellular residues involved in recognition of the eotaxin family of chemokines. Mol Immunol 43: 1221-2131, 2006.
34. van Aalst EJ, McDonald CJ and Wylie BJ: Cholesterol biases the conformational landscape of the chemokine receptor CCR3: A MAS SSNMR-filtered molecular dynamics study. J Chem Inf Model 63: 3068-3085, 2023.
35. Malgija MB, Rajendran HAD, Darvin SS, Nachimuthu S and Priyakumari J: In silico exploration of HIV entry co-receptor antagonists: A combination of molecular modeling, docking and molecular dynamics simulations. Acta Sci Pharm Sci 3: 60-67, 2019.
36. Manna M, Niemelä M, Tynkkynen J, Javanainen M, Kulig W, Müller DJ, Rog T and Vattulainen I: Mechanism of allosteric regulation of β_2-adrenergic receptor by cholesterol. Elife 5: e18432, 2016.